

## Structure and properties of $AlB_{12}$ -Al detonation coatings on Steel 45

Aleksandr Umanskyi<sup>1</sup>, Valery Muratov<sup>1</sup>, Vladimir Sheludko<sup>1\*</sup>, Konstantin Haltsov<sup>1</sup>, Aleksey Bondarenko<sup>1</sup>, Tatiana Mosina<sup>1</sup>, Vyacheslav Syrovatka<sup>1</sup>, Irina Martsenyuk<sup>1</sup>, Victor Varchenko<sup>1</sup>, Valery Kremenitsky<sup>2</sup>, Anatolii Minitskyi<sup>3</sup>, Aleksey Kushchev<sup>1</sup>

<sup>1</sup> Frantsevich Institute for Problems of Materials Science, NAS of Ukraine, 3 Omelyana Pritsaka (Krzhyzhanovsky) Str., 03142 Kyiv, Ukraine

<sup>2</sup> Technical Center, NAS of Ukraine, 13 Pokrovskaya Str., 04070 Kyiv, Ukraine

<sup>3</sup> National Technical University of Ukraine "Igor Sikorsky Kyiv Polytechnic Institute", 37 Beresteysky Ave., 03056 Kyiv, Ukraine  
v.sheludko@ipms.kyiv.ua

**Abstract:** The work is dedicated to the study of the properties of detonation coatings  $AlB_{12}$ -30 wt.% Al (AB70) applied to Steel 45 using the DNEPR-5M installation. The coatings have the following characteristics: thickness  $h \sim 170$ -200  $\mu\text{m}$ ,  $H_{\mu} = 27$ -29 GPa,  $HV = 4.35$  GPa. Changes in the tribological characteristics of the composite depending on the friction mode are analyzed. The AB70 coating is found to have stable tribological characteristics:  $f = 0.21$ -0.38, wear rate  $I = 3.3$ -8.6  $\mu\text{m}/\text{km}$ . Samples with coatings exceed uncoated Steel 45 in wear resistance. Changes in the surface structure after friction depending on the sliding speed and load are shown. Two wear mechanisms – oxidative and adhesive-abrasive – are established. A conclusion was drawn regarding the possibility of using the  $AlB_{12}$ -Al system to apply detonation coatings.

**KEYWORDS:**  $AlB_{12}$ -AL, DETONATION COATINGS, MICROSTRUCTURE, HARDNESS, X-RAY DIFFRACTION, SEM, TRIBOLOGICAL CHARACTERISTICS

### 1. Introduction

The properties of the working surfaces of parts and structural elements of machines and constructions are determining factors in their operational reliability and service life [1]. Increasing the service life of machine parts can be achieved by applying coatings on their surfaces protecting them from corrosion and erosion, wear, high-temperature action of aggressive environments, etc. [2-4].

In this regard, detonation spraying (D-spraying) has become widespread. This method is based on the principle of heating the sprayed material (usually a powder) followed by its acceleration and transfer to the sprayed part using the detonation products of gas-oxygen fuel (propane-butane or acetylene-oxygen mixtures are commonly used) [5]. Due to the high velocity of the sprayed particles (600-1000 m/s), D-coatings have minimal porosity (~1%) and significant adhesive strength (40-200 MPa) of the coating to the part, depending on the sprayed material. Moreover, heating of the sprayed product is insignificant (up to ~250°C), which helps prevent volumetric changes in the part. In addition, D-spraying is a very economical, but not very productive method (compared, for example, to high-velocity thermal spraying). As a rule, it is economical for spraying surfaces no more than a few square centimeters in area.

Detonation spraying allows to apply a wide range of materials: metals and alloys, oxides, their mixtures, hard metal-ceramic alloys based on tungsten carbides, chromium, titanium, mixtures of carbides with metals, as well as borides [1, 5, 6-10].

Among the latter, aluminum dodecaboride  $AlB_{12}$  is of interest. The method of its synthesis from Al and BN developed at the Frantsevich Institute for Problems of Materials Science of NAS of Ukraine, turn to be more rational and cost-effective than direct synthesis from Al and B [11].  $AlB_{12}$  has a low density (~2.52 g/cm<sup>3</sup>), and the particularity of its crystalline structure (icosahedral boron framework) determines its high hardness (22-24 GPa), and infusibility (2070 °C) [12].

However, the low crack resistance of aluminum dodecaboride significantly limits the scope of its application [12]; therefore, it is advisable to use  $AlB_{12}$  in combination with ductile bonded metal. It is promising to use aluminum, which is characterized by high plasticity, low density (2.7 g/cm<sup>3</sup>) and low melting point (660 °C). Al was found to wet  $AlB_{12}$  well with the formation of contact angles  $\Theta \approx 20$  deg, and there are no secondary phases in the interaction zone at the Al- $AlB_{12}$  interface [12]. In particular, the composite material  $AlB_{12}$ -50 wt.% Al was used in the deposition of electric spark coatings on titanium (VT1-0) and aluminum (D1) alloys, as well as on Steel 45 [13-15].

The aim of the work is to investigate the possibility of using the composite powder material "aluminum dodecaboride  $AlB_{12}$ -Al" to obtain D-coatings on Steel 45, and to investigate the structure and properties of these coatings.

### 2. Experimental

Powder materials used in this study were high-purity Al (99.8 %) and  $AlB_{12}$  produced by CVD method due to reaction of hexagonal boron nitride and aluminum:  $12BN + 13Al \rightarrow AlB_{12} + 12AlN$  [16]. The average size of  $AlB_{12}$  powder particles was 150±200 nm. The  $AlB_{12}$ -Al composite powder was produced by conglomerating the starting components in an organic binder (zapon) followed by sieving to obtain a particle size in the range of -63...+20  $\mu\text{m}$ . The resulting composition was  $AlB_{12}$ -30 wt.% Al, hereinafter referred to as AB70.

D-coatings were applied to a 1×1 cm Steel 45 (GOST 1050-88) substrate using a DNEPR-5M installation in the following mode: spraying distance  $L = 170$  mm, combustible mixture: acetylene  $C_2H_2$ /oxygen  $O_2 = 20/30$  g, frequency  $f = 4$  Hz, spraying time  $t = 10$  s.

The microhardness of the D-coatings was measured using a PMT-3 microhardness tester at a load of  $P = 0.5$  N. The Vickers hardness HV was measured using a FALCON500 stationary hardness tester (INNOVATEST, the Netherlands) at a load of  $P = 1.96$  N.

Tribological studies of the D-coatings were conducted on an M-22M friction machine in accordance with GOST 26614-85 under the following conditions:  $P = 2, 4,$  and 6 MPa,  $V = 2$  and 4 m/s, friction path  $S = 2$  km. Hardened Steel 45 (HRC 45-50) was used as the counterbody.

X-ray diffraction analysis of the D-coatings surface was performed on a Rigaku Ultima-IV diffractometer (Rigaku Corp., Tokyo, Japan) using  $CuK_{\alpha}$ -filtered radiation ( $\lambda = 1.54051 \text{ \AA}$ ).

The structure of the D-coatings was studied using a JEOL JSM-6490 LV SEM equipped with an INKA Energy 350XT energy-dispersive spectrometer (Oxford Instruments plc.) and a REM-106I SEM (JSC "SELMI", Sumy, Ukraine).

### 3. Results and discussion

The general view and microstructure of the AB70 D-coating cross-section are shown in Fig. 1. The average thickness is 170-200  $\mu\text{m}$ , and the microhardness is  $H_{\mu} = 27$ -29 GPa. However, there are also sections with  $H_{\mu} = 7$ -9 GPa and 0.9-2.8 GPa. The Vickers hardness, measured perpendicular and parallel to the coating thickness, averages  $HV = 4.35$  GPa.

The surface of the AB70 composite is uniform.  $AlB_{12}$  particles, 2.9-3.4  $\mu\text{m}$  in size, are evenly distributed within the  $Al_2O_3$  matrix. On the one hand, these particles adhere more tightly to the counterbody surface, increasing the tribocontact area, on the other hand they also promoting more intense oxidation with the formation of oxide layers. The periodic destruction of these layers reduces the strength of the microvolumes in the surface layer of the tribocontact, promoting oxidative wear.

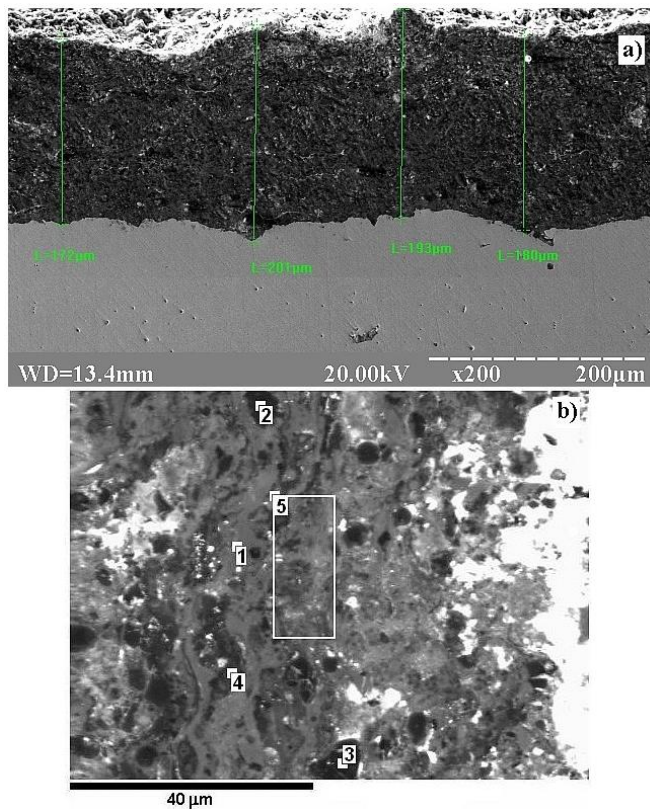


Fig. 1. Microstructure of the cross-section of the D-coating AB70 with the results of local elemental analysis: a – general view; b – cross-section

The results of the local elemental analysis of the AB70 D-coating and its phase composition are presented in Table 1 and Fig. 2. The data in Table 1 indicate that the composite contains regions with increased Al (~57 wt.%) and oxygen (~43 wt.%) contents. Boron is part of  $\text{AlB}_{12}$ , and oxygen and aluminum form secondary structures (mainly oxides) during friction.

Table 1. Results of local elemental analysis of AB70 D-coating (Fig. 1)

Spectrum	Element, wt.%				Total
	B	O	Al	C	
AB70 D-coating					
1		43.16	50.69	6.15	100
2	83.09		16.91		
3	81.87	0.61	17.52		
4	68.99	10.77	20.24		
5		32.89	57.11	8.67	

Elemental analysis confirms the presence of elements in the coating corresponding to the main phases (Al,  $\text{Al}_2\text{O}_3$ ,  $\text{AlB}_{12}$ , Fig. 2).

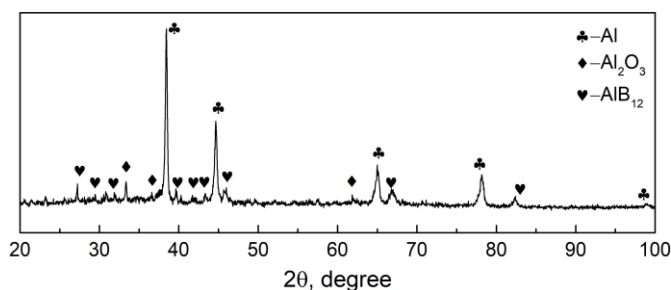


Fig. 2. Diffraction pattern of AB70 D-coating on Steel 45

Fig. 3 shows the results of tribological tests of AB70 samples in dry friction mode. These data indicate that with increasing load and sliding speed, the friction coefficient decreases and wear intensity increases. Compared to uncoated Steel 45, the AB70 composition exhibits significantly improved wear resistance. With increasing load to 6 MPa, the wear of uncoated Steel 45 becomes catastrophic.

Fig. 4a shows the surface of the AB70 coating after friction on Steel 45 ( $P = 2$  MPa,  $V = 4$  m/s). A characteristic feature is the presence of dark areas consisting of  $\text{AlB}_{12}$  aggregates penetrated by light particles (ranging in size from 3 to 6.2  $\mu\text{m}$ ). The light areas are represented by elongated conglomerates or individual grains. A characteristic feature is the presence of zones with a high oxygen content (up to 51.73 wt.%) and iron (up to 77.23 wt.%), which indicates the formation of Al and Fe oxides during friction (Table 2). Hard  $\text{AlB}_{12}$  fragments act as an abrasive on the counterbody surface, crushing and cutting off protrusions, facilitating the transfer of iron from the counterbody. Thus, areas with iron inclusions appear on the surface. Heating the surface ( $T \sim 230$  °C) during friction promotes the oxidation of Al and Fe, forming solid oxides that also contribute to abrasive wear. Thus, in this case, two conjugated wear mechanisms are present – oxidative and adhesive-abrasive.

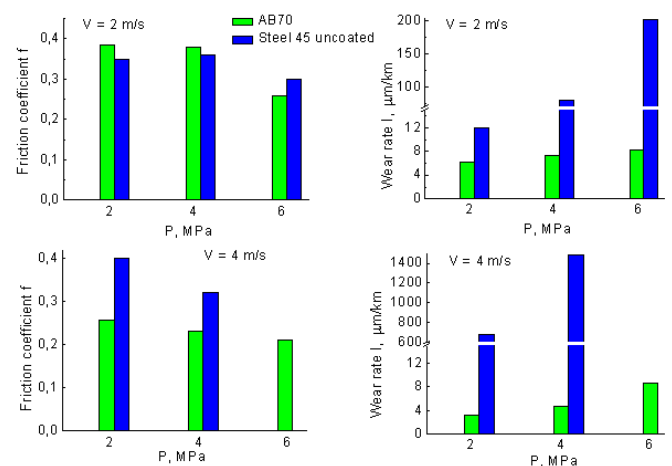


Fig. 3. Tribological characteristics of AB70 D-coating on Steel 45 and Steel 45 without coating under different loads and sliding speeds

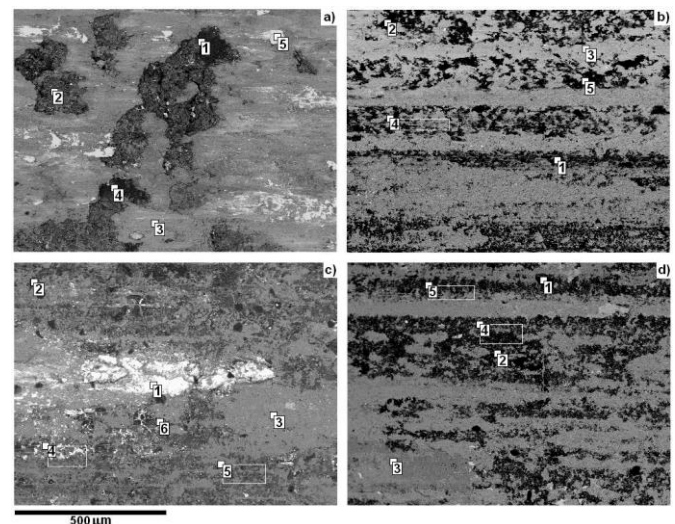


Fig. 4. Surface of the D-coating AB70 under friction on Steel 45 ( $V = 4$  m/s): a –  $P = 2$  MPa; b –  $P = 4$  MPa; c –  $P = 6$  MPa and d – surface of the AB70 coating under friction on steel ShKh15 ( $P = 6$  MPa,  $V = 6$  m/s) with the results of local elemental analysis

As the load increases to  $P = 4$  MPa at the same sliding speed, ordering of the relief occurs and alternating layers form (Fig. 4b). Layers with dark  $\text{AlB}_{12}$  inclusions (62 to 100  $\mu\text{m}$  in size) alternate with light layers 212 to 225  $\mu\text{m}$  in width. Local microanalysis data (Table 2) indicate that this mode results in the formation of larger  $\text{AlB}_{12}$  grains, distributed within the layers and between them as fine particles, covering the entire surface. As a result, the  $\text{AlB}_{12}$  particles exhibit a more intense abrasive effect, promoting the formation of iron in the contact zone, followed by the formation of complex  $\text{Al}_x\text{Fe}_y\text{O}_z$  oxides.

**Table 2.** Results of local elemental analysis of the friction surface of the AB70 D-coating (Fig. 4)

Spectrum	Element, wt.%									Total
	B	O	Al	C	Cr	Fe	Si	Mn	Ni	
Fig. 4a										
1	82.67	1.36	15.97							100.00
2		46.06	52.05	0.43	1.11	0.35				
3		51.73	20.93			27.34				
4	82.77	10.45	16.78							
5		21.09	0.93			77.23	0.75			
Fig. 4b										
1	81.49	1.89	16.62							100.00
2	81.72	0.73	17.01			0.54				
3		37.18	10.46			52.36				
4		40.01	28.67			31.32				
5	44.30	26.07	23.98			5.64				
Fig. 4c										
1		22.53	0.46			76.19		0.82		100.00
2	43.90	26.36	25.56			4.18				
3		44.21	18.72	4.44		32.63				
4		30.76	28.55	4.56	1.05	32.47			2.61	
5		45.04	37.35		1.22	16.39				
6	82.02	1.53	16.45							
Fig. 4d										
1	81.07	1.53	15.06						2.34	100.00
2	81.90	1.03	17.07							
3		43.88	15.56	3.79		36.77				
4		41.67	42.70			15.63				
5		40.43	46.07			13.50				

The system we consider as a frictional contact is dissipative and meets the criteria of self-organization (system openness, nonlinear processes of deformation and wear, formation of secondary structures, etc.). During friction, incoming energy is dissipated into other forms of energy, particularly heat, and accumulated by secondary structures, resulting in self-organization of the system. Furthermore, the principle of structural dissipation of accumulated energy into structural elements in the form of elastic energy is realized within them [17].

Like most structural materials, the composite under study is statistically nonuniform, which determines the nonlinearity of the deformation and wear processes during frictional interaction [18]. The authors [19, 20] note the role of secondary contact structures in the boundary layers of the metal during friction and wear. Such secondary structures can be oxide films in the boundary layers or a supersaturated oxygen solution in plastically deformed surface volumes of the metal, defects and damage of structures in the contact volumes, etc. [21]. During friction, as a result of the interaction of particles of the original disordered system, the deformation contact adapts to changing conditions (temperature, sliding speed, and load). The most important result of such adaptation is the self-organization (ordering) of the system, as a result of which the energy, force, tribomechanical parameters of friction and wear are reduced. These are friction coefficient, temperature, mass wear of the sample and wear intensity [19].

In our system, with a further increase in load to  $P = 6$  MPa, the surface morphology changes (Fig. 4c). The striped relief structure is transformed into a uniform surface with light gray and darker areas. The continuous  $AlB_{12}$  network includes individual dodecaboride grains ranging in size from 12.5 to 25  $\mu m$ . Note the high iron content at different points, ranging from 4.18 to 79.19 wt.% (Table 2). As a result of surface seizure followed by tear-out, a large elongated conglomerate consisting mainly of iron oxide  $FeO$  is formed. A more uniform contact surface aids in reducing the friction coefficient to  $f = 0.21$  and the abrasive effect of the resulting oxides increases the wear intensity (Fig. 3).

Any macroscopic system consists of a large number of microscopic states (e.g., volume, temperature, pressure, etc.), characterized by entropy. The evolution of a tribological system consists in achieving a state with entropy lower than its initial value

[22]. For example, if the system is heated from temperature  $T_1$  to  $T_2$ , the change in entropy  $\Delta S$  is expressed by the following expression [23]:

$$\Delta S_{1 \rightarrow 2} = S_2 - S_1 = \int_{1 \rightarrow 2} \frac{dQ}{T}, \quad (1)$$

where  $\frac{dQ}{T}$  – the reduced amount of heat imparted to the system during its transition from state 1 to state 2. Taking into account  $dQ = mc dT$ , where  $m$  is the mass of the sample,  $c$  is its specific heat capacity, formula (1) will take the form ( $T_1 = 298$  K):

$$\Delta S = mc \ln \left( \frac{T_2}{T_1} \right) \quad (2)$$

The data in Fig. 3 indicate that the AB70 sample is characterized by minimal values of tribotechnical characteristics compared to uncoated Steel 45, which is one of the external manifestations of self-organization [19]. At a load of  $P = 6$  MPa and a sliding speed of  $V = 4$  m/s, the result of self-organization of the system is not only a change (ordering) of the surface microgeometry (Fig. 4b, c), but also a decrease in the tribotechnical characteristics. Therefore, it was of interest to compare the change in entropy during friction of a sample with and without a coating. The calculation was carried out using formula (2) and the results are presented in Table 3. Analysis of the change in  $\Delta S$  indicates that at  $V = 4$  m/s and  $P = 2$  and 4 MPa, the change in entropy during friction of the AB70 composite is 137 and 114 times less than during friction under the same conditions of uncoated Steel 45, which confirms the assumption of self-organization of the system during friction.

**Table 3.** Results of entropy calculation  $\Delta S$ 

Friction mode	Sample temperature $T_2$ , K		Entropy $\Delta S$ , J/K	
	AB70-coated Steel 45	Uncoated Steel 45	AB70-coated Steel 45	Uncoated Steel 45
$P = 2$ MPa $V = 4$ m/s	500	471	0.00338	0.4654
$P = 4$ MPa $V = 4$ m/s	610	496	0.00462	0.5283

Analyzing the data in Fig. 4, one can note the following sequence of changes in the tribocontact relief and wear mechanisms depending on the friction mode.

The friction process at  $P = 2$  MPa and  $V = 4$  m/s is characterized by two conjugated wear mechanism: oxidative and adhesive-abrasive. As the load increases to 4 MPa at the same speed, the microgeometry of the relief changes toward ordering (self-organization). Layers with larger grains of hard  $AlB_{12}$  can move over layers with fine particles, reducing the friction coefficient. The composite structure contains zones with increased oxygen and iron content due to the formation of oxides through the oxidative wear mechanism. The presence of  $AlB_{12}$  aggregates does not exclude the possibility of abrasive wear, which results in the formation of iron in the contact zone.

With increasing load to 6 MPa, a continuous, uniform relief is formed with dispersed  $AlB_{12}$  grains with increased oxygen, aluminum, and iron content, as well as particles of the oxide layer (Table 2), indicating an oxidative wear mechanism. In this case, the influence of temperature, which contributes to oxidative wear, cannot be excluded, since in this mode the temperature in the tribocontact zone is  $\sim 360$  °C.

It is of interest to compare the obtained data with the results of friction in contact with a harder counterbody. Fig. 4d shows the surface of the AB70 coating during friction on ShKh15 ball bearing steel, the hardness of which (HRC61-63) exceeds the hardness of Steel 45 counterbody. The tests were carried out under more severe conditions ( $P = 6$  MPa,  $V = 6$  m/s). The AB70 coating remained resistant to this mode. At friction on a harder counterbody, a less ordered surface structure is formed with wider bands, which mainly contain aluminum, oxygen, and iron. The iron content is lower (from 13.5 to 36.77 wt.%, Table 2), since the harder counterbody is less susceptible to the abrasive action of  $AlB_{12}$  and complex oxides. Increasing the hardness of the counterbody makes difficult plastic deformation and micro-cutting of the friction surface. At that, the friction coefficient  $f = 0.24$ , the mass wear of the sample increased slightly to 2.8 mg/km, while that of the counterbody decreased to 0.18 mg/km. The wear rate of the friction pair is  $I = 8.2$   $\mu\text{m}/\text{km}$ . Increasing the temperature in the contact zone to  $T = 432$  °C promotes intensification of oxidation processes with the formation of complex oxides  $Al_xFe_yO_z$  and the transition to oxidative wear mode.

#### 4. Conclusions

For the first time, using D-spraying, a coating of the  $AlB_{12}$ -Al system with different contents of boride and aluminum components was obtained ( $AlB_{12}$ -30 wt.% Al (AB70)), and some of its properties such as thickness  $h = 170$ -200  $\mu\text{m}$ , microhardness  $H_{\mu} = 27$ -29 GPa, Vickers hardness  $HV = 4.35$  GPa were determined. The  $AlB_{12}$ -Al system can be used to produce D-coatings on steels.

Tribological tests of the coatings were conducted at sliding speeds  $V = 2, 4,$  and 6 m/s and loads  $P = 2, 4,$  and 6 MPa. The AB70 composition has the following characteristics:  $f = 0.21$ -0.38,  $I = 3.3$ -8.6  $\mu\text{m}/\text{km}$ .

The structure of the surface layer changes depending on the sliding speed: the alternating strip relief at  $V = 4$  m/s is transformed into a uniform surface at  $V = 6$  m/s, which indicates the processes of ordering (self-organization) of structures in the contact zone with a decrease in the entropy value.

Based on the results of local microanalysis, the formation of iron and aluminum oxides in the friction zone was established. This

indicates an oxidative wear mechanism, and the appearance of iron in the contact zone confirms adhesive-abrasive wear as a result of the impact of solid  $AlB_{12}$  particles and oxides on the surface of the counterbody.

By replacing the counterbody material with harder hardened ShKh15 steel, the coating proved resistant to severe friction conditions:  $f = 0.24$ ,  $I = 8.2$   $\mu\text{m}/\text{km}$ . The counterbody's mass wear rate was decreased by approximately 35 times (to 1.8 mg/km).

#### 5. References

1. P.A. Vityaz', A.F. Il'ushchenko, A.I. Shevtsov, *Fundamentals of Applying of Wear-, Corrosion-resistant and Heat-shielding Coatings* (Bel. Nauka, Minsk, 2006) [in Russian]
2. Virupakshappa Lakkannavar, K.B. Yogesha, C. Durga Prasad et al., *Results Surf. Interfaces*, **16**, 100250 (2024)
3. H. Bai, L. Zhong, L. Kang et al., *J. Alloys Compd.*, **882**, 160645 (2021)
4. T. Hoornaert, Z.K. Hua, and J.H. Zhang, *Proc. of CIST2008 & ITS-IFTtoMM2008*, Beijing, China, 24-27 September 2008.– PP. 774–779
5. A. Hasui, *Spray-Coating Technique*. [Russian Translation] (Mashinostroenie, Moscow, 1975)
6. J. Keränen, T. Stenberg, T. Mäntylä et al., *Surf. Coat. Technol.*, **82**(1-2), 29 (1996)
7. Gao Yang, Hei Zu-kun, Xu Xiaolei, and Xin Gang, *J. Therm. Spray Technol.*, **10**(3), 456 (2001)
8. H. P. Lv, J. Wang, Y. G. Yan et al., *Mater. Sci. Technol.*, **26**(8), 950 (2010)
9. Lakhwinder Singh, Vikas Chawla, J.S. Grewal, *J. Miner. Mater. Charact. Eng.*, **11**(3), 243 (2012)
10. V.P. Konoval, O.P. Umanskyi, O.A. Bondarenko et al., *Powder Metall. Met. Ceram.*, **59**(5-6), 308 (2020)
11. O.O. Vasiliev, V.B. Muratov, T.I. Duda, *Phys. Chem. Solid St.*, **18**(3), 358 (2017)
12. P.S. Kisly, V.A. Neronov, T.A. Prikhna et al., *Aluminum Borides* (Nauk. Dumka, Kiev, 1990) [in Russian]
13. A.P. Umanskyi, M.S. Storozhenko, V.E. Sheludko et al., *Funct. Mater.*, **28**(4), 694 (2021)
14. A.P. Umanskyi, M.S. Storozhenko, V.E. Sheludko et al., *Metallophys. Adv. Technol.*, **43**(11), 1443 (2021)
15. A.P. Umanskyi, A.I. Dukhota, V.E. Sheludko et al., *Funct. Mater.*, **29**(4), 514 (2022)
16. UA Patent 107193 (2016)
17. S.V. Fedorov, E. Assenova, *J. of Science and Education of North-West Russia*, **3**, 1 (2017) [in Russian]
18. A.G. Kuzmenko, *Problems of Tribology*, **3**, 106 (2012) [in Russian]
19. D.M. Baranovskiy, *Eastern-European J. of Enterprise Technologies*, **3/8(39)**, 28 (2009) [in Ukrainian]
20. O.A. Mikosianchyk, R.G. Mnatsakanov, V.I. Kalinichenko et al., *Problems of Tribology*, **3**, 6 (2016) [in Russian]
21. M.I. Denysenko, O.V. Zazimko, V.F. Labunets et al., *Problems of Friction and Wear*, **4(69)**, 38 (2015) [in Russian]
22. V.V. Aulin, *Physical fundamentals of processes and states of self-organization in tribotechnical systems* (KOD, Kirovograd, 2014) [in Ukrainian]
23. D.V. Sivukhin, *General Course of Physics*. In 5 vols. V. II. *Thermodynamics and Molecular Physics* (FIZMATLIT, Moscow, 2005) [in Russian]